ISSN 0030-400X, Optics and Spectroscopy, 2021, Vol. 129, No. 6, pp. 612–621. © Pleiades Publishing, Ltd., 2021.
ISSN 0030-400X, Optics and Spectroscopy, 2021. © Pleiades Publishing, Ltd., 2021.
Russian Text © The Author(s), 2021, published in Optika i Spektroskopiya, 2021, Vol. 129, No. 5, pp. 541–549.

Spectral-Luminescent Properties and Photolysis of Charged Forms of Bisphenol A

E. N. Bocharnikova[a], *, O. K. Bazyl'[a], O. N. Tchaikovskaya[a], and G. V. Mayer[a]

[a] *National Research Tomsk State University, Tomsk, 634050 Russia*

**e-mail: bocharnikova.2010@mail.ru*

Received November 2, 2020; revised December 11, 2020; accepted January 29, 2021

Abstract—Spectral-luminescent properties and photolysis of charged forms (cation and anion) of bisphenol A are studied experimentally and by methods of quantum chemistry. The calculations and the experiment demonstrate that no new absorption bands appear in the absorption spectra of charged forms in the region of 200–600 nm as compared to a neutral molecule. The polar solvent (water) shifts the absorption spectrum bands of the ionic forms to the region of low energies. In this case, the shift of cation absorption spectrum is insignificant, while the shift of anion absorption spectrum is significant as the intensity of absorption bands increases. The low quantum yield of fluorescence of ionic forms is explained by the predominance of singlet-triplet conversion efficiency over the efficiency of the radiation channel of fluorescent state decay. The low quantum yield of fluorescence of the anion form is due not only to the effective singlet-triplet conversion, but also to the low efficiency of the radiation decay of the fluorescent state of the anion caused by a change in its orbital nature. Calculations demonstrate that the potential curves of the excited states of bisphenol A and its ionic forms have a significant potential barrier for photolysis. An increase in the potential reaction barrier in the cation decreases the efficiency of its photolysis. The increase in the photodissociation efficiency of the bisphenol A anion is caused by a noticeable decrease in the potential barrier and an increase in the overlap between the absorption spectra of the bisphenol A anion and the solar radiation.

Keywords: cation, anion, bisphenol A, spectral-luminescent properties, quantum chemistry, photolysis

DOI: 10.1134/S0030400X21050040

INTRODUCTION

Most scientific reports on the study of bisphenol A (BPA) concern its synthesis [1], obtaining polycarbonate from BPA [2], its toxicity to living organisms [3, 4], and methods of its utilization [5–12]. Moreover, the mechanism of photochemical transformation of BPA is unconfirmed. In [13], the authors used the semiempirical PM3 method to find agreement with the experimental data on the position of the first absorption band and the photoluminescence maxima of synthesized BPA-based dyes. According to the authors, the results obtained may be of considerable interest for the development of new effective organic phosphors technology for electroluminescent applications. In [14], an attempt to interpret the peaks in the BPA spectrum in the region of 400–4000 cm^{-1} using the density functional theory (DFT) with the B3LYP 6-311G++(3df 3pd) configuration was presented.

BPA is a well-known endocrine disruptor with devastating estrogen-like side effects. It causes undesirable effects on humans and wildlife. According to available data on BPA toxicity, its concentration level is 1 μg/L in fresh water [15] but can reach 17.2 μg/L in the landfill filtrate. In this regard, the question of finding a way to effectively remove BPA from wastewater before it is discharged into natural waters remains topical. The literature most often contains publications on BPA photodegradation under the action of various sources using UV/H_2O_2 and photocatalysis technologies [16–19]. However, photocatalytic oxidation often does not result in BPA reduction, and conventional biological treatment at wastewater treatment plants is not effective in removing BPA from wastewater. In this regard, further study of the BPA phototransformation mechanism remains topical.

Studying the influence of the molecular structure on the reactivity of neutral and ionized molecules is of considerable scientific and practical interest [20–23]. The basic idea of studies of the spectra of organic molecules is based on the fact that optical spectra are related in a certain way to the spatial and electronic structure of molecules the combination of which just determines their various properties. One way to study physicochemical properties and their changes is through the spectra of electronic absorption and fluorescence of the systems under study. However, in a series of cases, the solution to this problem cannot be obtained only on an experimental basis, and the dependence of the electronic structure of a molecule

on its structure can only be correctly obtained using quantum chemistry methods. Present-day quantum chemical methods are effectively used for studying the geometrical and electronic structures of organic molecules, as well as the influence of these characteristics on their reactivity. The goal of our research is the ways for effective BPA disruption under the action of sunlight in order to reduce the harmful BPA effect on the environment and humans.

RESEARCH TECHNIQUES

Experimental Methods

Absorption spectra of neutral and charged BPA forms were recorded on a Cary-500 Scan UV-Vis-NIR spectrophotometer (Varian, USA) [24] in distilled water, as well as in the presence of acid HCl and alkali NaOH at a concentration of 10^{-4} mol/L at room temperature in the range of 200–600 nm. All measurements were performed according to the standard technique in a quartz cuvette with an optical path length of 10 mm. The compound under study is moderately soluble in water (6 g of the substance per 100 g of water).

Using derivative spectrophotometry, bands that appear only as hidden maxima and fuzzy kinks in the absorption spectrum were isolated [25]. The quantum yield of fluorescence (γ) was determined by the relative method. As a reference, BPA in water was chosen ($\gamma = 0.001$) [26].

Quantum-Chemical Calculations, Comparison with the Experiment

Spectral-luminescent characteristics of molecules are a reflection of peculiarities of their electron shell structure determined by the chemical structure of the compound. The main objective of studies of spectral-luminescent properties of molecules is to establish the relationship between these properties and the chemical and electronic structure of the objects under study. In this investigation, the semiempirical method of intermediate neglect of differential overlap (INDO) and the package of quantum-chemical programs created in the department of photonics of the Siberian Physical Technical Institute at Tomsk State University based on the method are used. The software package we use, together with the original parametrization [27], is oriented to the study of photonics of organic polyatomic molecules. This software package calculates the energy of molecular orbitals (MOs), energy, and intensity of electronic transitions. The analysis of coefficients of the expansion of molecular orbitals in atomic orbitals allows one to determine the orbital nature and localization of electronic transitions, i.e., to interpret absorption spectra of organic molecules. The software system calculates the electron density distribution on atoms and chemical bonds of the molecule under study, as well as its dipole moments in the ground and excited states.

The main difference between the described software package based on the INDO method and similar ones is the possibility to calculate the rate constants of emissive (k_r) and nonradiative (constants of internal k_{ic} and singlet-triplet k_{ST} conversion) processes in polyatomic molecules. The rate constants of nonradiative processes were calculated according to the technique [28], they are of an estimative character, and allow one to establish not only the trend of the fluorescence quantum yield $\gamma = k_r/(k_r + k_{ic} + k_{ST})$ in series of similarly constructed molecules but also to establish the cause of the absence of the fluorescence process. This software system calculates spectra of singlet and triplet electronically excited states both of neutral and of charged forms of molecules.

Correctness of the calculation of absorption spectra is estimated by comparison with experimental spectra of solutions by the position of the maximum of absorption spectrum bands and by the value of the molar extinction coefficient at the maximum of these bands; correctness of the electronic charge distribution is estimated by comparison with the dipole moment of the molecule in the ground state if experimental data are available. The calculated spectrum of an isolated molecule is compared with the spectrum in a nonpolar solvent. Correctness of conclusions regarding the fluorescence spectra is controlled by the experimentally measured band positions and the quantum yield of the process. The geometry of the studied structures was calculated using averaged values of chemical bond lengths and valence angles according to [29]. To calculate charged forms and complexes, the package used includes a program for calculating the molecular electrostatic potential (MEP) [30, 31], which makes it possible to determine the most electron-acceptor center of the molecule and the most probable site of proton attachment. In the case of the BPA molecule, these centers are the oxygen atoms of the hydroxyl groups. The results of MEP calculation were used in modeling both the BPA + $2H_2O$ complex and the BPA + $2H^+H_2O$ double-charged cation (Fig. 1b). The BPA cation was modeled by a complex with a hydrogen bond between the BPA molecule and a proton solvated by a water molecule.

The anionic form of BPA is formed when one or two protons are detached from hydroxyl groups. This results in the formation of a single- or double-charged ion. We considered the single-charged ion (Fig. 1c) under the assumption that its formation more likely because it requires less energy for breaking one of the O–H bonds. The better agreement of the calculated absorption spectrum of the single-charged ion with the experimental spectrum corroborated our assumption. Calculation of the ion structure shows that about 80% of the negative charge of the anion is concentrated at the oxygen atom of the hydroxyl group with

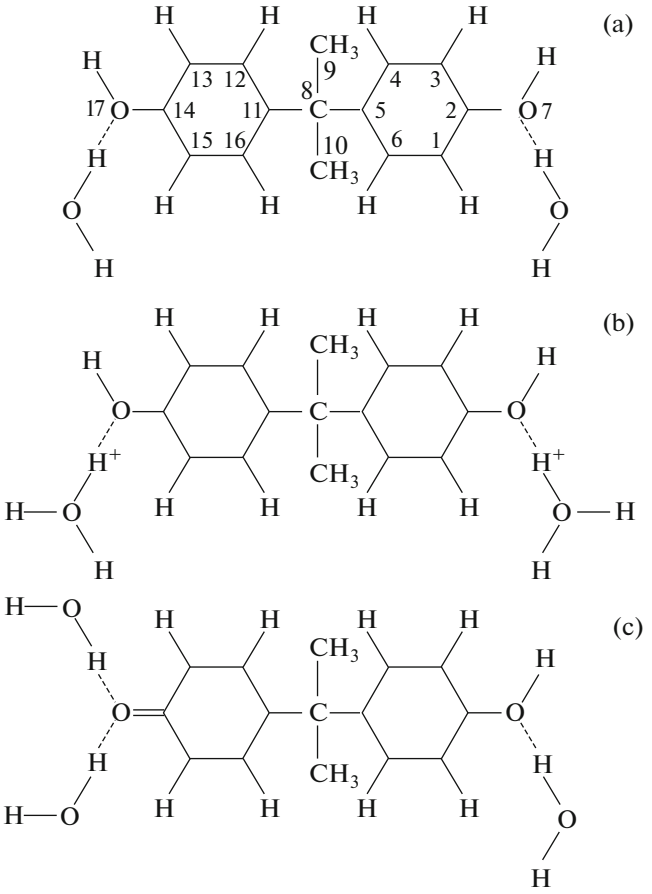

Fig. 1. Structure formulas of the (a) neutral BPA complex with water with composition of 1 : 2, (b) BPA cation ($q = +2e$), and (c) $+2H_2O$ anion ($q = -1e$).

the detached proton (O_7 or O_{17}, Fig. 1). The two unseparated pairs of electrons of the oxygen atom remaining after the O–H bond is broken form two MEP minima, which allows two neutral water molecules to be attached to the oxygen atom (Fig. 1c).

To correctly calculate the fluorescence spectrum, we took into account the change in the chemical bond lengths of the molecule in the fluorescent state with respect to the ground state which is determined from the change in the electronic density (population) of the chemical bond according to Mulliken [32] by the dependence

$$\Delta R^*(\mathrm{AB}) = k\Delta P^*(\mathrm{AB}),$$

where ΔP^*(AB) is the change in the population of the bond AB when passing to the fluorescent state; the value of coefficient $k = 0.46$ was obtained from the change in the length of the C–C bond of benzene in the transition $S_0 \rightarrow S_1$ [33].

The approach we proposed earlier in [34, 35] to the study of chemical bond photobreaking in the electronically excited states is as follows. Chemical bond breaking occurs in the $\pi\sigma^*$, $\sigma\pi^*$, and $\sigma\sigma^*$ states because the σ–σ bonds constituting the structure core of the molecule can be broken only in states of this type. The possibility of bond breaking in any electronic state of the abovementioned type is evidenced by the decrease in the strength of the bond under study.

The potential curve of the ground state of the molecule was modeled by the Morse potential [36]:

$$E(R) = D(e^{-2\alpha} - 2e^{\alpha}),$$

where $\alpha = vR_0\sqrt{M/2D}$. The bond dissociation energy (D), the equilibrium length of the bond under study (R_0), the oscillation frequency (ω), and the reduced mass of the oscillator (M) are taken from the experiment. The length of the bond investigated for breaking is varied and, at each step, the energy of the excited state localized at the bond under study is calculated. Then, the potential curve of the excited state under study is plotted. The shape of the potential curve is used to judge whether the bond is broken or, on the contrary, whether it is stable.

RESULTS AND DISCUSSION

Electronic Absorption Spectra of Charged BPA Forms

The influence of different solvents (water, methanol, diethyl ether, *n*-hexane, cyclohexane, and mixtures) and excitation energy on the fluorescence quantum yield of compounds (phenol, anisole, *p*-cresol, *p*-methylanisole, 3,5-dimethylphenol, and 2,4,6-trimethylphenol) was studied by the authors of [37, 38]. It was found that the fluorescence quantum yield of the compounds in nonpolar solvents and in water decreased markedly. The authors suppose that one of the causes for this behavior is the participation of OH-groups. The formation of hydrogen bonds between the molecules of the abovementioned compounds and water leads to an increase in the nonradiative transitions. The proton–acceptor equilibrium of hydroxy compounds was studied in [39–42]. The authors note that photoexcitation of molecules leads to significant changes in their electronic structure and reactivity associated with proton addition or detachment. It has been shown that at neutral pH values, hydroxy compounds in water exist in ionic forms in the ground and excited states. In this study, we assume that BPA in water can also exist in ionic forms.

Figure 2 presents the absorption spectra; Fig. 3, the fluorescence spectra of BPA and its charged forms in water—cation and anion—in the region from 200 nm. The absorption spectrum of BPA in water was modeled in calculations by a hydrogen-bonded complex of the composition 1 : 2 with the distance between oxygen atoms of BPA molecules and water equal to 2.7 Å, the average value of this parameter in complexes with a hydrogen bond of the –HO...H–OH type bond [43].

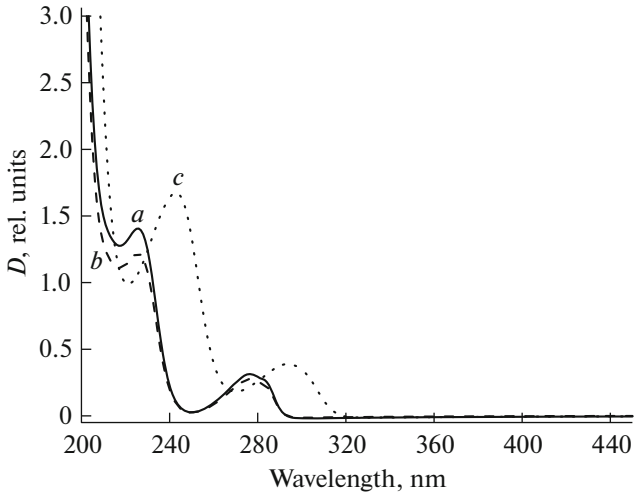

Fig. 2. BPA absorption spectra in the aqueous solution at pH (*a*) 5.6, (*b*) 1, and (*c*) 10.11.

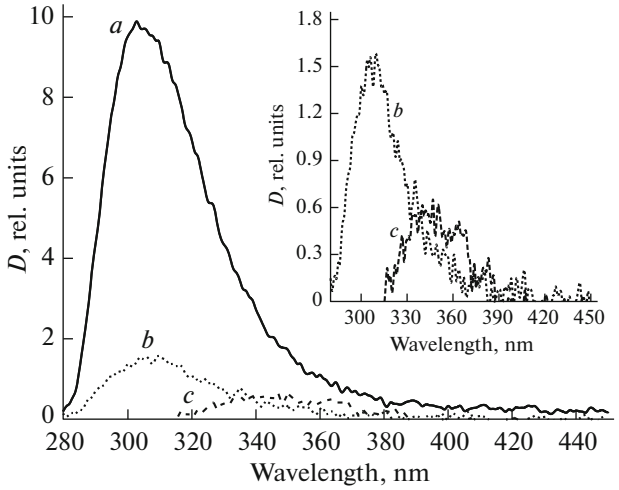

Fig. 3. BPA fluorescence spectra in the aqueous solution at pH (*a*) 5.6, (*b*) 1, and (*c*) 10.11.

As follows from the form of the BPA spectrum in water at pH 5.6 (Fig. 2, curve *a*), it contains two absorption bands. Processing of the absorption spectrum using the second derivative method gives two electronic transitions of 36200 and 35090 cm^{-1} for the longwave band and one for the band in the region of 43700 cm^{-1}. Comparison performed earlier [44] for the absorption spectra in hexane and water showed that the formation of the hydrogen-bonded complex in an aqueous solution of BPA (BPA + $2H_2O$) in fact did not change the position of the longwave band and its intensity but shifted the band with a maximum at 43 700 cm^{-1} towards low energies. In addition, it was noted that the longwave band includes an electronic transition $S_0 \rightarrow S_3$ ($\pi\sigma^*$) the σ^*-orbital of which is localized at the C_5–C_8–C_{11} bond (Fig. 1). Earlier, it was shown [45] that it is the electronic transition that is responsible for the break of one of BPA bonds (C_5–C_8 or C_8–C_{11}).

Comparison of the absorption spectra of the BPA + $2H_2O$ complex and the BPA + $2H^+H_2O$ cation (q = +2e) reveals their almost complete identity: two absorption bands in the region of 36200 and 43700 cm^{-1} (Fig. 2). Analysis of the calculation results shows a significant difference only in the populations (strengths) of ordinary BPA bonds. In particular, the formation of a cation carrying a charge +2e in the state S_6 ($\pi\sigma_{5-8-11}$) strengths the C_5–C_8 and C_8–C_{11} bonds and weakens the C_8–C_9 and C_8–C_{10} bonds. However, in S_3 ($\pi\sigma^*$) state, the C_5–C_8 and C_8–C_{11} bonds remain weaker. The population of these bonds in the BPA + $2H^+H_2O$ cation in the ground and first singlet excited states insignificantly differs from the population of the same bonds in the complex with water (Table 1).

As for the strength of the O–H bond, it increases in the cation as compared to the BPA + $2H_2O$ complex and is almost unchanged in all states presented in Table 1. This fact indirectly corroborates that this group does not take part in the formation of absorption spectrum bands of the BPA cation in the spectral range of >200 nm.

Considerably greater differences with respect to the spectrum of the BPA + $2H_2O$ complex take place in the absorption spectrum of the BPA anion (Table 2). It is known that the isolated BPA molecule is nonplanar [44, 45], and its complex with water and its charged forms are also nonplanar (Fig. 1a). The core of the BPA molecule consists of two identical phenol fragments connected by the $C(CH_3)_2$ group; the planes of benzene rings are at an angle to each other. The middle fragment of the $C(CH_3)_2$ molecule prevents the appearance of π-conjugation between the phenyl rings, which leads to the existence of two isolated π-systems in the BPA molecule. The nonplanar structure of BPA also leads to a strong "mixing" of atomic wave functions of π- and σ-types. Therefore, referring an electronic state to a particular orbital type ($\pi\pi^*$, $\pi\sigma^*$, or $\sigma\sigma^*$) is conventional depending on the contribution of the corresponding MOs in the configurations forming one or another electronic state.

Orbital mixing of $\pi\pi^*$- and $\pi\sigma^*$-states manifests itself in the orbital nature of excited states of the singly charged BPA + $2H_2O$ anion. In contrast to two previous structures, the S_1 state of which is classified as the $\pi\pi^*$-type state, the orbital nature of the S_1 state of the BPA anion is "mixed" (Table 2). In addition, more than 50% belong to the configuration of the $\pi\sigma^*$-type the atomic orbital σ^* of which is localized at the C_5–C_8 and C_8–C_{11} bonds.

Table 1. Populations (P_{AB}) of ordinary bonds in the complex with water and in charged forms of bisphenol A

State	P_{AB} of C–C bonds, e				P_{AB} of O–H bonds, e	
	P_{5-8}	P_{8-11}	P_{8-9}	P_{8-10}	P_{2-7}	P_{14-17}
BPA complex + $2H_2O$						
S_0	0.781	0.796	0.685	0.683	0.578	0.583
S_1 ($\pi\pi^*$)	0.754	0.792	0.677	0.675	0.578	0.588
S_3 ($\pi\sigma^*_{5-8-11}$)	0.232	0.242	0.389	0.409	0.578	0.583
BPA cation + $2H^+H_2O$ ($q = +2e$)						
S_0	0.795	0.786	0.684	0.684	0.655	0.656
S_1 ($\pi\pi^*$)	0.772	0.774	0.679	0.675	0.660	0.669
S_3 ($\pi\sigma^*_{5-8-11}$)	0.292	0.298	0.440	0.489	0.665	0.663
BPA anion + $2H_2O$ ($q = -1e$)						
S_0	0.794	0.790	0.695	0.683	0.674	0.745
S_1 ($\pi\pi^* + \pi\sigma^*_{5-8-11}$)	0.233	0.504	0.425	0.446	0.661	0.655
S_2 ($\pi\pi^*$)	0.771	0.785	0.676	0.660	0.670	0.685

The absorption spectrum of the anion is bathochromically shifted (Fig. 2, curve *c*) relative to the BPA spectra in water at pH 5.6 and 1 (Table 2). The absorption spectrum of the BPA anion in the region of >280 nm overlaps with the spectrum of solar radiation (>300 nm). Probably, this leads to an increase in the absorption of solar radiation by the BPA anion and to a higher probability of the break of one of the single C–C bonds (C_5–C_8 or C_8–C_{11}), i.e., the bond from which the proton is detached during the formation of the singly charged anion. As for the strength of the broken bond in the anion, according to calculations it changes little in comparison with the BPA + $2H_2O$ complex in the ground and $\pi\pi^*$-states but is less strong in comparison with the BPA + $2H^+H_2O$ cation in the $\pi\sigma^*_{5-8}$-state. The strength of the C–C(CH_3) bonds also decreases (Table 2) but remains noticeably stronger than the C_5–C_8 and C_8–C_{11} bonds in the $\pi\sigma^*$ state localized at these bonds.

According to the experimental data, the longwave absorption band of the BPA + $2H^+H_2O$ cation is shifted to the longwave region by only ~100 cm^{-1} (Fig. 2). Taking into account that the strength of the broken C_5–C_8 bond in the cation is higher than in the anion (Table 2), one should not expect an increase in the efficiency of C_5–C_8 bond breaking in the cationic BPA form. Comparison of the calculation results with the experiment (Table 2) for the recorded absorption bands of the charged BPA forms demonstrates a satisfactory agreement of the calculation with the experiment. According to the calculations, the longwave absorption band at ~36200 nm in all structures is formed by several electronic transitions, mainly of the $\pi\pi^*$-type, which form the band intensity. Similarly, the ~43700 nm band is formed (Table 2). Analysis of the orbital nature of the electronic transitions in the region of 200–600 nm shows that the electronic transitions forming the absorption of these two bands in the absorption spectrum are localized on phenyl rings. The hydroxyl and CH_3 groups of the central fragment of the molecule do not participate in the formation of electronic transitions in the region of bands of 36200 and 43700 cm^{-1}.

Fluorescence Spectra of Charged BPA Forms

BPA weakly fluoresces both in hexane and in water. Since the absorption spectra of BPA and solar radiation have little overlap, fluorescence of the aqueous BPA solution was excited at the edge of the longwave absorption band of the molecule. The fluorescence band maximum of the isolated molecule (solution in hexane) in the experiment lies at ~300 nm (33300 cm^{-1}) [34, 36]. The fluorescence band maximum of the aqueous BPA solution (BPA + $2H_2O$ complex) is located at ~306 nm (32300 cm^{-1}). Table 3 presents the calculated fluorescence characteristics for aqueous solutions of BPA and its charged forms in comparison with the experiment. It follows from the tables that the calculation results for the charged forms of BPA and experiment coincide satisfactorily in the position of the fluorescence band and worse in the fluorescence quantum yield. The latter may be related to the failure

Table 2. Experimental and theoretical characteristics of absorption spectra of the complex with water and charged BPA forms in water

Calculation				Experiment		
State	E_i, cm^{-1}	λ_i, nm	f	E_i^{max}, cm^{-1}	λ, nm	ε, l/mol cm
BPA complex + $2H_2O$ (neutral form)						
$S_1(\pi\pi^*)$	34040	294	0.054	35090	285	2000
$S_2(\pi\pi^*)$	34990	286	0.048	36200	276	3000
$S_3(\pi\sigma^*_{5-8-11})$	36890	271	0.012			
$S_4(\pi\pi^*)$	38090	262	0.244			
$S_9(\pi\pi^*)$	44700	224	0.071	43700	229	15000
$S_{11}(\pi\pi^*)$	45340	220	0.509			
$S_{12}(\pi\pi^*)$	45805	218	0.552			
BPA cation (BPA + $2H^+H_2O$, $q = +2e$)						
$S_1(\pi\pi^*)$	34640	289	0.040	35200	284	2000
$S_2(\pi\pi^*)$	35720	280	0.048	36200	276	3000
$S_3(\pi\sigma^*_{5-8-11})$	38510	242	0.035			
$S_4(\pi\pi^*)$	39680	252	0.256			
$S_5(\pi\pi^* + \pi\sigma^*)$	44660	224	0.140	43700	229	11000
$S_6(\pi\pi^*)$	45540	220	0.854			
BPA anion + $2H_2O$ ($q = -1e$)						
$S_1(\pi\pi^* + \pi\sigma^*_{5-8})$	33200	301	0.020	33100	302	4000
$S_2(\pi\pi^*)$	33530	298	0.106			
$S_3(\pi\pi^*)$	35460	282	0.065	34300	292	5000
$S_6(\pi\pi^* + \pi\sigma^*_{5-8})$	39250	255	0.211	40500	247	20000
$S_8(\pi\pi^*)$	41190	243	0.086			
$S_{13}(\pi\pi^*)$	43680	229	0.244			

E_i is the energy of the purely electron transition, f is the oscillator force of this transition, λ is the wavelength of the purely electron transition, and ε is the molar extinction coefficient of the absorption band.

to take into account some of decay channels of the fluorescent state of the molecules. According to calculations, the main reason for the low fluorescence quantum yield of the BPA + $2H_2O$ complex (Table 3) is the effective singlet–triplet conversion process in the $S_1(\pi\pi^*) \rightsquigarrow T_n(\pi\sigma^*)$ channel.

It follows from data of Table 3 that in all the structures considered, the efficiencies of the nontradiative channels of the fluorescent state decay are close, while the efficiencies of the radiation channel differ more significantly. The calculated anionic form has the lowest fluorescence quantum yield (Table 3). This is caused by the change in the orbital nature of the fluorescent state of the anion form as compared to other structures studied. The fact is that the orbital nature of the S_1 state of the anion is mixed and consists of $\pi\pi^*$-and $\pi\sigma^*$-type configurations, where the contribution of the $\pi\sigma^*$-type configuration exceeds that of the $\pi\pi^*$-type configuration. The small oscillator strength of the $S_0 \rightarrow S_1$ transition (Table 2) leads to a small rate constant of radiative decay, which, along with the high rate constant for singlet–triplet conversion, just gives an anion quantum yield equal to ~10^{-5}.

Photolysis of Charged BPA Forms

In quantum chemical calculations, the electron density is distributed between atoms of the molecule

Table 3. Calculated and experimental characteristics of BPA fluorescence, BPA complex with water, and BPA charged forms

Calculation					Experiment	
E_{fl}, cm^{-1} (nm)	k_r, s^{-1}	k_{ic}, s^{-1}	k_{ST}, s^{-1}	γ	E_{fl}, cm^{-1} (nm)	γ
BPA						
$S_1(\pi\pi^*)$ 33020 (303)	6×10^7	5×10^3	3×10^{10}	0.002	33300 (300)	0.001 [26]
BPA complex with water (BPA + $2H_2O$)						
$S_1(\pi\pi^*)$ 32520 (308)	4×10^7	2×10^4	3×10^{10}	0.001	32700 (306)	0.0005
BPA cation (BPA + $2H^+H_2O$), ($q = +2e$)						
$S_1(\pi\pi^*)$ 34540 (290)	2×10^7	3×10^3	2×10^{10}	0.001	32300 (310)	0.0001
BPA anion + $2H_2O$ ($q = -1e$)						
$S_1(\pi\sigma^*)$ 26660 (275)	3×10^5	8×10^3	4×10^{10}	$\sim 10^{-5}$	28800 (350)	0.00006

and bonds between them. The value of the electron density on the bond and the population of the bond indicate the strength of the chemical bond. An increase in the bond population indicates its strengthening (an increase in bonding energy); a decrease, on the contrary, indicates its weakening (a decrease in its energy). As follows from comparison of population of bonds between atoms of the same type, such as carbon atoms, single C–C bonds are less strong. It follows from data in Table 1 that the C–(CH_3) and OH bonds in the ground state are the weakest in the BPA molecule; in the πσ*-type states, however, the C_5–C_8 and C_8–C_{11} bonds turn out to be weaker. Moreover, as mentioned above, the C–(CH_3) and O–H bonds do not take part in the formation of electronically excited states forming the absorption in the spectral range of >200 nm. It also follows from data in Table 1 that single bonds in this molecule under excitation change differently depending on the orbital nature of the excited state. The greatest decrease in bond strength is characteristic of the C_5–C_8 and C_8–C_{11} bonds in the states localized on these bonds. In the positively charged BPA form, the C_5–C_8 and C_8–C_{11} bonds are somewhat strengthened; in the anion, populations of bonds in the OH group from which the proton is detached (C_5–C_8 or C_8–C_{11}) do not change as compared to populations of these bonds in the analogous excited state of the BPA + $2H_2O$ complex. Table 1 presents the bond populations only in the singlet states. A similar trend also holds for triplet states of similar orbital nature and localization.

The Morse potential curve for the C_5–C_8 (or C_8–C_{11}) bond was constructed using the following experimental values: the equilibrium bond length $R_0 = 1.5$ Å [44], the dissociation energy of the ordinary C–C bond $D = 346$ kJ/mol [46], and $\omega = 1000$ cm^{-1} [47]. The calculated potential curves of singlet excited states of different forms of the BPA molecule are presented in Fig. 4, where the length of the C_8–C_{11} (or C_5–C_8) bond is taken as the reaction coordinate; it varied from 1.5 to 3.0 Å.

Earlier studies of the photolysis of polyatomic organic molecules showed that the molecule was stable in various compounds in the ππ*-type states [34, 35]. The same is true for the isolated BPA molecule, its BPA + $2H_2O$ complex [44], and charged BPA forms. The character of the potential curves of ππ*-type states of the complex and the charged BPA forms is similar to the character of the curves of this type in the previously studied molecules [34, 35]; for this reason, the potential curves of the ππ*-type structures under study are not shown in order to avoid overloading of the figure. The potential curves of πσ*-type states localized at one of the breakable bonds (C_5–C_8 or C_8–C_{11}) of BPA have a significant potential barrier to photolysis. Nevertheless, the authors [48] experimentally discovered by liquid chromatography in deionized water a product of BPA degradation under sunlight irradiation the formation of which is possible only when one of BPA bonds (C_5–C_8 or C_8–C_{11}) is broken.

Potential curves of the photodissociative states of charged forms have the following potential barriers: ~12100 cm^{-1} for the BPA + $2H^+H_2O$ cation, which is higher by ~1000 cm^{-1} than for the BPA + $2H_2O$ complex, and ~9700 cm^{-1} for the anion, which is lower by ~3000 cm^{-1} than the potential barrier for photolysis of the BPA + $2H_2O$ complex. The shape of the potential curve of the S_1 state ($\pi\pi^* + \pi\sigma^*_{5-8}$) of the anion differs from similar curves of the BPA + $2H^+H_2O$ cation and the BPA + $2H_2O$ complex by the absence of the drop of the potential curve of the photodissociative state with the growth of the length of the broken bond.

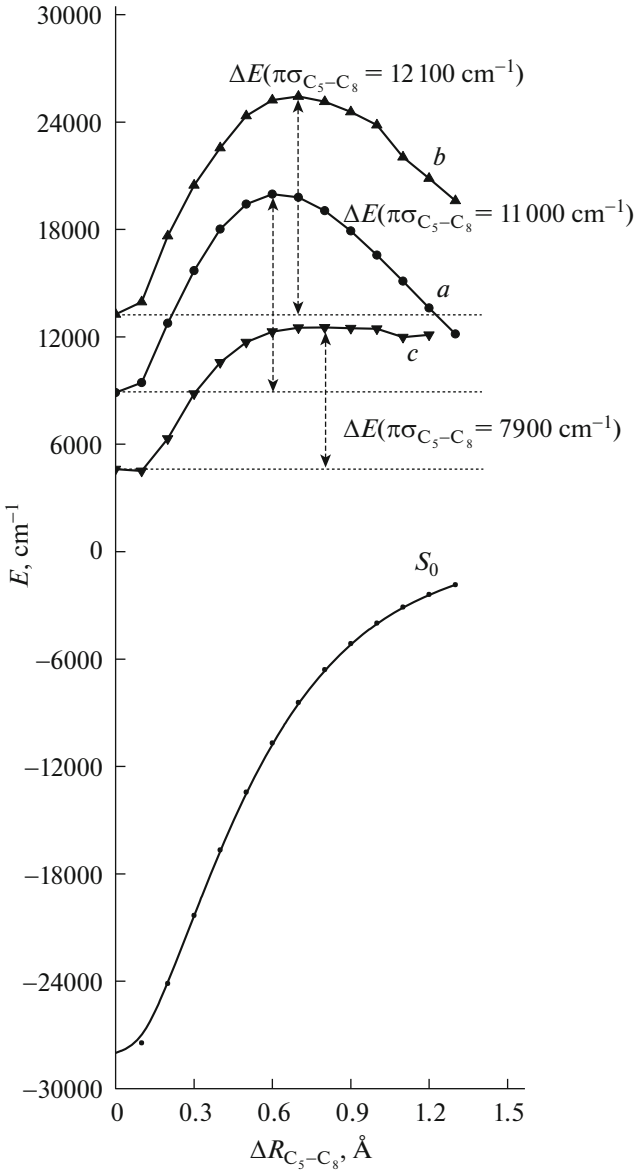

Fig. 4. Potential curves of the ground and excited photodissociative states of the (a) BPA + $2H_2O$ complex, (b) cation, and (c) BPA + $2H_2O$ anion. ΔE is the potential barrier of the photolysis.

However, such facts as (i) a significant increase in the overlap of the absorption spectra of the BPA anion and solar radiation, which increases the amount of absorbed energy, (ii) decrease in the strength of the broken bond in the photodissociative state, and (iii) decrease in the potential barrier of the photodissociative state in comparison with the potential barrier of the BPA + $2H_2O$ complex (Fig. 4) suggest that the probability of photodetachment of the C_8–C_{11} (or C_5–C_8) bond in ionic BPA forms fits into the following series: anion > isolated molecule > BPA + $2H_2O$ complex > BPA + $2H^+H_2O$ cation. Note that the authors [49] demonstrated that ozonation of the BPA solution facilitated the process of its photolysis when the solution is alkalized to pH 10.8, i.e., with the formation of the BPA anion.

CONCLUSIONS

It has been established experimentally that absorption spectra of charged forms contain no new absorption bands in the region of 200–600 nm as compared to the neutral form. Absorption spectra of ionic BPA forms are shifted to the longwave region in relation to the neutral form: insignificantly in the case of the cation and noticeably longer for the anion with an increase in the intensity of absorption bands.

The low fluorescence quantum yield of BPA and its ionic forms in water is caused by the significant predominance of the singlet–triplet conversion channel over the channel of radiation decay of the fluorescent state. The nonplanar structure of BPA and its charged forms leading to mixing of ππ*- and πσ*-type orbitals, which is typical of the fluorescent anion state, leads to a noticeable decrease in the radiation decay efficiency of the anion form and, together with the singlet–triplet conversion, to the lowest fluorescence quantum yield among the considered structures.

Quantum chemical calculations demonstrate that the efficiency of BPA cation photolysis under the action of solar radiation is lower than in the case of the BPA + $2H_2O$ complex, as a consequence of an increase in the potential barrier. The efficiency of anion photolysis should be expected to be higher than that of the cation and complex with water due to a decrease in the potential barrier, as well as an increase in the overlap of the absorption spectra of the anion and the solar radiation.

FUNDING

This work was supported by the Ministry of Science and Higher Education of the Russian Federation, contract no. 0721-2020-0033 for 2020–2024.

CONFLICT OF INTEREST

The authors declare that they have no conflicts of interest.

REFERENCES

1. A. Factor and M. L. Chu, Polym. Degrad. Stab. **2**, 203 (1980). https://doi.org/10.1016/0141-3910(80)90029-4
2. C. Lu, J. Li, Y. Yang, and J.-M. Lin, Talanta **82**, 1576 (2010). https://doi.org/10.1016/j.talanta.2010.07.052
3. Y. Nakagawa and S. Tayama, Arch. Toxicol. **74**, 99 (2000). https://doi.org/10.1007/s002040050659

4. C. A. Pryde and M. Y. Hellman, J. Appl. Polym. **25**, 2573 (1980). https://doi.org/10.1002/app.1980.070251114
5. D. Zhou, F. Wu, N. Deng, and W. Xiang, Water Res. **38**, 4107 (2004). https://doi.org/10.1016/j.watres.2004.07.021
6. Yu-P. Chin, P. L. Miller, L. Zeng, K. Cawley, and L. K. Weavers, Environ. Sci. Technol. **38**, 5888 (2004). https://doi.org/10.1021/es0496569
7. J. López-Cervantes and P. Paseiro-Losada, Food Addit. Contam. **20**, 596 (2010). https://doi.org/10.1080/026520031000109495
8. E. J. Rosenfeldt and K. G. Linden, Environ. Sci. Technol. **38**, 5476 (2004). https://doi.org/10.1021/es035413p
9. B. Wang, F. Wu, P. Li, and N. Deng, React. Kinet. Catal. Lett. **92**, 3 (2007). https://doi.org/10.1007/s11144-007-5045-0
10. E. Felis, S. Ledakowicz, and J. S. Miller, Water Environ. Res. **83**, 2154 (2011). https://doi.org/10.2175/106143011X12989211841214
11. R. A. Torres, C. Pétrier, E. Combet, F. Moulet, and C. Pulgarin, Environ. Sci. Technol. **41**, 297 (2007). https://doi.org/10.1021/es061440e
12. Z. Guo, Q. Dong, D. He, and C. Zhang, Chem. Eng. J. **183**, 10 (2012). https://doi.org/10.1016/j.cej.2011.12.006
13. E. Gondek, A. Danel, B. Kwiecień, J. Nizioł, and A. V. Kityk, Mater. Chem. Phys. **119**, 140 (2010). https://doi.org/10.1016/j.matchemphys.2009.08.048
14. R. Ullah, I. Ahmad, and Y. Zheng, J. Mol. Struct. **1108**, 649 (2016). https://doi.org/10.1155/2016/2073613
15. Environment Canada, Health Canada, Chemical Abstracts Service CAS 80-05-7 (Canada, 2008).
16. P. J. Chen, K. G. Linden, D. E. Hinton, S. Kashiwada, E. J. Rosenfeldt, and S. W. Kullman, Chemosphere **65**, 1094 (2006). https://doi.org/10.1016/j.chemosphere.2006.04.048
17. M. F. Brugnera, K. Rajeshwar, J. C. Cardoso, and M. V. Boldrin Zanoni, Chemosphere **78**, 569 (2010). https://doi.org/10.1016/j.chemosphere.2009.10.058
18. S.-H. Yoon, S. Jeong, and S. J. Lee, Environ. Technol. **33**, 123 (2012). https://doi.org/10.1080/09593330.2011.579181
19. E. N. Bocharnikova, O. N. Tchaikovskaya, V. S. Chaidonova, M. Gomez, M. Murcia, and J. L. Gomez, IOP Conf. Ser.: Mater. Sci. Eng. **696**, 012006 (2019). https://doi.org/10.1088/1757-899X/696/1/012006
20. D. W. Kolpin, E. T. Furlong, M. T. Meyer, E. M. Thurman, S. D. Zaugg, L. B. Barber, and H. T. Buxton, Environ. Sci. Technol. **36**, 1202 (2002). https://doi.org/10.1021/es011055j
21. G. M. Khrapkovskii, D. D. Sharipov, A. G. Shamov, D. L. Egorov, D. V. Chachkov, B. Nguyen Van, and R. V. Tsyshevsky, Comput. Theor. Chem. **1017**, 7 (2013). https://doi.org/10.1016/j.comptc.2013.04.013
22. C. C. J. Roothaan, Rev. Mod. Phys. **23**, 69 (1951). https://doi.org/10.1103/RevModPhys.23.69
23. Studies Org. Chem. **51**, 38 (1996). https://doi.org/10.1016/S0165-3253(96)80008-3
24. E. S. Voropai, M. P. Samtsov, A. E. Rad'ko, K. N. Kaplevskii, P. P. Pershukevich, M. V. Bel'kov, and F. A. Ermalitskii, in *Laser and Optoelectronic Technology, Collection of Articles* (Akad. Upr. Prezid. RB, Minsk, 2006), No. 10, p. 200 [in Russian].
25. M. I. Bulatov and I. P. Kalinkin, *A Practical Guide to Photometric Methods of Analysis* (Khimiya, Leningrad, 1986) [in Russian].
26. E. M. Sokolov, L. E. Sheinkman, and D. V. Dergunov, Voda: Khim. Ekol., No. 4, 26 (2012). https://doi.org/10.18412/1816-0395-2012-4-36-39
27. V. Ya. Artyukhov and A. I. Galeeva, Sov. Phys. J. **29**, 949 (1986). https://doi.org/10.1007/BF00898453
28. G. V. Mayer, V. G. Plotnikov, and V. Ya. Artyukhov, Russ. Phys. J. **59**, 513 (2016). https://doi.org/10.1007/s11182-016-0801-0
29. A. I. Kitaigorodskii, P. M. Zorkii, and V. K. Bel'skii, *The Structure of Organic Matter (Data from Structural Studies 1929–1970)* (Nauka, Moscow, 1980) [in Russian].
30. E. Scroco and J. Tomasi, Adv. Quantum Chem. **11**, 115 (1978). https://doi.org/10.1016/S0065-3276(08)60236-1
31. V. Ya. Artyukhov, J. Struct. Chem. **19**, 364 (1978). https://doi.org/10.1007/BF00753260
32. R. S. Mulliken, J. Chem. Phys. **23**, 1833 (1955). https://doi.org/10.1063/1.1740588
33. G. Herzberg, *Molecular Spectra and Molecular Structure. III. Electronic Spectra and Electronic Structure of Polyatomic Molecules* (Krieger, Malabar, 1991).
34. N. A. Borisevich, A. Ya. Gorelenko, N. S. Lysak, S. V. Mel'nichuk, S. A. Tikhomirov, V. A. Tolkachev, and G. B. Tolstorozhev, JETP Lett. **43**, 145 (1986).
35. O. K. Bazyl', V. Ya. Artyukhov, G. V. Maier, and I. V. Sokolova, High Energy Chem. **34**, 30 (2000).
36. H. Wang, Y. H. Zhao, Y. J. Zhu, and J. Y. Shen, Vacuum **128**, 198 (2016). https://doi.org/10.1016/j.vacuum.2016.03.015
37. G. Köhler and N. Getoff, J. Chem. Soc. Faraday Trans. **72**, 2101 (1976). https://doi.org/10.1039/F19767202101
38. G. Köhler and N. Getoff, Chem. Phys. Lett. **26**, 525 (1974). https://doi.org/10.1016/0009-2614(74)80406-9
39. Yu. P. Morozova, O. N. Chaikovskaya, and N. Yu. Vasil'eva, Russ. J. Phys. Chem. A **72**, 210 (1998).
40. O. N. Chaikovskaya, I. V. Sokolova, and T. V. Sokolova, J. Appl. Spectrosc. **72**, 172 (2005). https://doi.org/10.1007/s10812-005-0050-4
41. O. K. Bazyl, V. Ya. Artyukhov, O. N. Chaikovskaya, and G. V. Maier, Opt. Spectrosc. **97**, 552 (2004). https://doi.org/10.1134/1.1813696

42. O. N. Tchaikovskaya, T. V. Sokolova, O. K. Bazyl', and I. V. Sokolova, Russ. Phys. J. **48**, 300 (2005).

43. *Chemist's Handbook,* Vol. 1: *Basic Properties of Inorganic and Organic Compounds* (Khimiya, Moscow, Leningrad, 1964), p. 377.

44. O. K. Bazyl', E. N. Bocharnikova, and O. N. Chaikovskaya, Russ. Phys. J. **63**, 1403 (2020). https://doi.org/10.17223/00213411/63/8/102

45. E. N. Bocharnikova, O. N. Tchaikovskaya, O. K. Bazyl, V. Ya. Artyukhov, and G. V. Mayer, Adv. Quantum Chem. **81**, 191 (2020). https://doi.org/10.1016/bs.aiq.2019.12.001

46. B. R. Eggins, *Chemical Structure and Reactivity* (Macmillan, New York, 1972).

47. L. Bellamy, *The Infrared Spectra of Complex Molecules* (Chapman and Hall, London, 1975).

48. M. Mezcua, J. Ferrer, M. D. Hernando, and A. R. Fnandez-Alba, Food Addit. Contam. **23**, 1242 (2006). https://doi.org/10.1080/02652030600889541

49. I. Gultekin, V. Mavrov, and N. H. Ince, J. Adv. Oxid. Technol. **12**, 242 (2009). https://doi.org/10.1515/jaots-2009-0215

Translated by A. Nikol'skii